Schizophrenia Bulletin vol. 43 no. 4 pp. 914–924, 2017
doi:10.1093/schbul/sbw145
Advance Access publication November 21, 2016

Consistent Functional Connectivity Alterations in Schizophrenia Spectrum Disorder: A Multisite Study

Kristina C. Skåtun[1], Tobias Kaufmann[1], Nhat Trung Doan[1], Dag Alnæs[1], Aldo Córdova-Palomera[1], Erik G. Jönsson[1,2], Helena Fatouros-Bergman[2], Lena Flyckt[2], KaSP[†]; Ingrid Melle[1], Ole A. Andreassen[1], Ingrid Agartz[1–3], and Lars T. Westlye[1,4,*]

[1]NORMENT, KG Jebsen Centre for Psychosis Research, Division of Mental Health and Addiction, Oslo University Hospital & Institute of Clinical Medicine, University of Oslo, Oslo, Norway; [2]Department of Clinical Neuroscience, Centre for Psychiatric Research, Karolinska Institutet, Stockholm, Sweden; [3]Department of Psychiatric Research, Diakonhjemmet Hospital, Oslo, Norway; [4]Department of Psychology, University of Oslo, Oslo, Norway

*To whom correspondence should be addressed; Oslo University Hospital HF, Division of Mental Health and Addiction, Psychosis Research Unit/TOP, Ullevål Hospital, Building 49, PO Box 4956 Nydalen, N-0424 Oslo, Norway; tel: +47-23027350, fax: +47-23027333, e-mail: l.t.westlye@psykologi.uio.no

[†]Members of Karolinska Schizophrenia Project (KaSP) are listed in the acknowledgments as collaborators.

Schizophrenia (SZ) is a severe mental illness with high heritability and complex etiology. Mounting evidence from neuroimaging has implicated disrupted brain network connectivity in the pathophysiology. However, previous findings are inconsistent, likely due to a combination of methodological and clinical variability and relatively small sample sizes. Few studies have used a data-driven approach for characterizing pathological interactions between regions in the whole brain and evaluated the generalizability across independent samples. To overcome this issue, we collected resting-state functional magnetic resonance imaging data from 3 independent samples (1 from Norway and 2 from Sweden) consisting of 182 persons with a SZ spectrum diagnosis and 348 healthy controls. We used a whole-brain data-driven definition of network nodes and regularized partial correlations to evaluate and compare putatively direct brain network node interactions between groups. The clinical utility of the functional connectivity features and the generalizability of effects across samples were evaluated by training and testing multivariate classifiers in the independent samples using machine learning. Univariate analyses revealed 14 network edges with consistent reductions in functional connectivity encompassing frontal, somatomotor, visual, auditory, and subcortical brain nodes in patients with SZ. We found a high overall accuracy in classifying patients and controls (up to 80%) using independent training and test samples, strongly supporting the generalizability of connectivity alterations across different scanners and heterogeneous samples. Overall, our findings demonstrate robust reductions in functional connectivity in SZ spectrum disorders, indicating disrupted information flow in sensory, subcortical, and frontal brain regions.

Key words: psychosis/brain networks/resting-state fMRI/independent component analysis/machine learning

Introduction

Schizophrenia (SZ) is a severe psychiatric illness characterized by hallucinations, delusions, apathy, social withdrawal, and impaired cognitive function.[1] Evidence from neuroimaging studies points to brain "dysconnectivity" in SZ,[2] possibly partly reflecting altered neurotransmission mediated by excitatory and inhibitory imbalances, including NMDA/glutamate and GABA dysfunction stemming from a combination of genetics, obstetric complications, neurodevelopmental perturbation, and altered synaptic plasticity.[3] Associations between disrupted spine density at the microscale and connectivity disruptions at the neuroimaging scale[4] support a link between the various levels of explanation. At the functional neuroimaging level, such neuromodulatory abnormalities may manifest as alterations in brain connectivity or integration of large-scale functional brain networks.[2,5] The relative contribution of specific networks may mirror the neuroanatomical distribution of the relevant gene expression patterns[6] or transmitters systems, reflecting primary deficits, or reflect secondary downstream or compensatory effects in distant networks.

In line with this, studies have reported altered brain networks in SZ,[5,7] including a wide range of large-scale brain networks, such as the default mode network (DMN)[8] and frontal regions,[9] which are critical for introspection/self-referential thought and cognitive functions. In SZ patients, studies have indicated aberrant connectivity between the DMN, the central executive network (involved in goal-oriented cognitive functions), and the salience network (detection of behaviorally relevant stimuli),[10–12] which could reflect or even modulate the ability to separate external information from self-generated thoughts.

Low-level sensory networks have been less extensively studied in SZ, but evidence points to a general reduced connectivity in these regions.[13–15] Auditory, visual, and somatomotor processes have been implicated in SZ,[16,17] and may be related to the range of cognitive and emotional symptoms through various downstream mechanisms (so-called bottom-up models).[18,19] Thalamic dysfunction has classically been involved in cognitive dysmetria or mental coordination models of SZ.[20] Also, the sensory gating hypothesis,[21] describing the filtering process by which the brain assigns relevance to external stimuli, strongly implicates aberrant thalamic functioning in SZ,[22,23] and thalamic synchronization with frontal and somatosensory regions[24,25] may reflect reduced dynamic flow and integration of information in the brain.

Despite both theoretical and methodological advances, functional connectivity findings vary across studies.[26] This heterogeneity likely reflects a combination of methodological and clinical variability, which have precluded a direct generalization across studies, and there is a need for well-powered studies applying common tools across independent samples.

In order to address the above-mentioned limitations and assess the robustness of brain network alterations in SZ, we utilize resting-state functional magnetic resonance imaging (rs-fMRI) data from 3 samples, including 182 SZ spectrum patients and 348 healthy controls (HC). We use a data-driven and anatomically unconstrained approach for defining network nodes across the brain in combination with partial correlations to assess connectivity strength between nodes. Using a combination of univariate and multivariate techniques, we compare the strength of the connections between patients and controls, and test for associations with key clinical variables. Next, we assess the generalizability using a machine-learning approach that allows us to train and test a multivariate classifier using independent samples. By assessing the accuracy of individual prediction of diagnosis, we test the clinical utility of the approach.

Based on a current conceptualization of the brain-network underpinnings of SZ, which suggest reduced network efficiency[27] and specifically implicate the cortico-cerebellar-striatal-thalamic loop and altered interaction between task-positive and task-negative networks in SZ,[28] we hypothesize the connectivity between these nodes to be affected with a general trend towards reduced connectivity. In addition, based on the conception that clinical symptoms and cognitive impairments represent higher-order consequences of basic sensory and perceptual dysfunctions, we expected sensory networks to be equally affected as higher order cognitive networks, with a reduced connectivity with other sensory regions and an increased coupling with the thalamus. Moreover, we expected frontal, DMN, and sensory nodes to show a high cumulative effect and be affected in several edges in SZ. Lastly, in line with the assumption that fMRI-based functional brain connectivity is a sensitive and robust intermediate phenotype for psychotic disorders, we expected that the multivariate classifier trained on one sample would perform reasonably well in the independent datasets.

Methods

Participants

Three samples were recruited; 1 from the University of Oslo, Norway and 2 from Karolinska Institutet, Stockholm, Sweden (table 1). Norwegian datasets were recruited through the TOP study,[7,14] and included 277 HC and 96 patients, with subgroups of SZ ($n = 50$), schizoaffective (SA, $n = 15$), schizophreniform (SFF, $n = 5$), and psychosis not otherwise specified (NOS, $n = 26$). Karolinska Schizophrenia Project (KaSP) consisted of 30 HC and 52 recently diagnosed patients (25 SZ, 3 SA, 15 psychosis NOS, 6 delusional disorder, 3 brief psychotic disorder), while Human Brain Informatics (HUBIN)[29] comprised 34 patients (9 SA, 23 SZ, 2 psychosis NOS) and 41 HC from a 12-year follow-up. For simplicity, all patients will be referred to as SZ, unless stated otherwise. Written informed consent was obtained from all participants, and the studies were approved by the regional ethics committees.

Patients were diagnosed using the structured clinical interview for DSM-IV (SCID). Symptom severity was assessed with Positive and Negative Syndrome Scale (PANSS)[30] in TOP and KaSP, and with the Scale for Assessment for Positive Symptoms (SAPS) and the Scale for Assessment for Negative Symptoms (SANS)[31,32] in HUBIN. Medication usage was operationalized as the defined daily dose (DDD) according to the guidelines provided by the World Health Organization (http://www.whocc.no/atcddd). The number of unmedicated patients was 6 in TOP and 29 in KaSP sample. HC were assessed with the Primary Care Evaluation of Mental Disorders (PRIME-MD)[33] in TOP, by a structured clinical interview in HUBIN,[34] and by the Mini-International Neuropsychiatric Interview[35] in KaSP.

Image Acquisition

All subjects underwent rs-fMRI and structural scans at a 3T General Electric scanner, either in Oslo or Stockholm. Imaging parameters are detailed in supplementary material.

Table 1. Demographic and Clinical Characteristics

	TOP		KaSP		HUBIN	
	SZ	HC	SZ	HC	SZ	HC
Demographics						
N	96	277	52	30	34	41
Age, y	28.7 (7.9)	31.9 (7.6)[a]	30 (8.6)	27.3 (5.8)	51.4 (8.2)	54.4 (8.9)
Sex, *n* (% male)	62 (64.6)	164 (59.2)	33 (63.5)	15 (50)	27 (79.4)	26 (63.4)
Education, y	12.6 (2.4)	14.5 (2.1)[a]	—	—	12.7 (2.2)	14.6 (2.8)[a]
IQ[b]	99.3 (15.4)	112.6 (10.7)[a]	—	—	92.3 (16.3)	106.2 (14.3)[a]
Duration of illness, y	5.8 (0.7)	—	1.34 (1.7)	—	28 (8.5)	—
Symptom rating						
PANSS total	58.2 (13.6)	—	74.4 (20.7)	—	—	—
PANSS positive	13.5 (5)	—	18.8 (6.1)	—	—	—
PANSS negative	14.9 (4.9)	—	17.4 (7.3)	—	—	—
SANS	—	—	—	—	29.3 (14.9)	—
SAPS	—	—	—	—	8.8 (7.5)	—
Antipsychotics DDD	1.31 (1.2)	—	1.11 (.7)	—	1.26 (.8)	—

Note: DDD, defined daily dose; IQ, intelligence quotient; PANSS, Positive and Negative Syndrome Scale; SAPS, Scale for Assessment for Positive Symptoms; SANS, Scale for Assessment for Negative Symptoms. Means (SDs) are reported unless otherwise specified. At the time of investigation, the number of unmedicated patients was 6 schizophrenia (SZ) patients in the TOP sample, and 29 in the KaSP sample. Number of missing data TOP: Education: 20 SZ, 37 controls; IQ: 17 SZ, 36 controls; duration of illness: 15 SZ; PANSS: 11 SZ; medication: 25 SZ. Missing data KaSP: duration of illness: 9 SZ; PANSS: 2 SZ, medication: 4 SZ. Missing data HUBIN: IQ: 10 SZ, 13 controls; medication: 4 SZ.
[a]Significant difference between the means of patients and controls within each sample.
[b]IQ was measured using Wechsler Abbreviated Scale of Intelligence.

Data Cleaning and Motion

In order to minimize confounding effects of motion and other sources of noise we performed single subject independent component analysis (ICA) and applied FMRIB's ICA-based Xnoiseifier (FIX) with a standard training set, which regresses out the components classified as noise and the estimated motion parameters from the fMRI data[36,37] (supplementary table S1). FIX has been shown to compare favorably to other methods.[38,39] We assessed the effects of denoising by calculating the proportion of noise and variance removed, and the temporal signal-to-noise ratio (tSNR)[40] before and after FIX. A repeated measures ANOVA was used to test for main and interactive effects of denoising (pre and post FIX) and group (SZ and HC) on tSNR (supplementary table S1). Moreover, we tested for group differences of head motion (defined as the average root mean square of the frame-to-frame displacement), and to which degree motion and tSNR influenced the main effects of group (see Statistical analysis). In addition, we tested for main effects of tSNR (post-FIX) on connectivity within HC on edges showing effects of group.

Preprocessing

Full brain segmentation[41] of the T1-weighted data was performed using FreeSurfer[42] to provide brain extracted structural volumes used for co-registration. fMRI datasets were processed using FEAT, part of FSL,[43] including brain extraction, motion correction, spatial smoothing using a Gaussian kernel of full-width at half-maximum (FWHM) of 6 mm, and a high-pass filter of 100 seconds. fMRI volumes were registered to the structural scan using FLIRT[44] and boundary-based registration,[45] the structural scan was nonlinearly warped to the Montreal Neurological Institute MNI152 template[46] using FNIRT,[43] before the same warping was applied to the fMRI data.

Independent Component Analysis

To integrate fMRI data obtained from 2 different scanners, we employed a meta-ICA approach.[47] Briefly, we randomly selected 140 subjects from each site and ran 2 decompositions per site (model order 80), each including 35 patients and 35 controls. A common brain mask containing voxels with signal in all subjects was used. The resulting group-level ICA spatial maps were used as input for a single-session meta-ICA[47] with a model order of 80. We used dual regression to estimate individual component time series and spatial maps using the group-level meta-ICA components as spatial regressors.[48,49] Components clearly associated with motion, white matter, CSF, or scanner artifacts were removed (supplementary figure S1). Due to the restricted brain coverage, the cerebellum components were excluded, leaving 59 components for further analysis (supplementary figure S2).

Connectivity Matrices

In line with recent studies,[14,50–52] we defined the components' spatial maps as nodes in the brain network,

and the estimated temporal associations between nodes as edges. Full correlations measure the temporal association between 2 components' time series, while partial correlations additionally control for the common influences from other components.[53,54] Partial correlations may thus provide a more "direct" measure[54] while also correcting for non-neural physiological noise.[55,56]

After regressing out the time series from noise-components, we computed connectivity matrices defined as the *z*-normalized node-by-node regularized partial correlations using custom Matlab (The Mathworks Inc) tools and FSLnets (http://fsl.fmrib.ox.ac.uk/fsl/fslwiki/FSLNets), yielding individual connectivity matrices comprising 1711 unique edges. In line with recent studies,[53,57] regularization was performed with an individual estimation of lambda.[58,59]

Statistical Analysis

For visualization purposes, the full correlation matrix averaged across subjects was used to compute a hierarchical clustering of the components (supplementary figure S3). To test for effects of diagnosis on edge connectivity, we ran ANCOVAs with diagnosis as independent variable, and age, sex, and site as covariates. Results were corrected at the FDR[60] and Bonferroni-level ($P < .05/1711$). For significant edges, we also tested if group effects were present within samples.

To assess the importance of each network node in distinguishing between cases and controls, we calculated the eigenvector centrality of each node based on the edgewise *F*-values from the group ANOVA. A high centrality indicates altered connectivity with several other nodes, indicating a relative importance of this node in group discrimination.

Multivariate Analysis—Machine Learning

We assessed the generalizability of the discriminative patterns across samples using regularized linear discriminant analysis classifiers[58,61] on edgewise connectivity.[14,57,62] First, we trained a binary classifier on TOP to discriminate HC from SZ and tested the classifier on HUBIN, KaSP and the HUBIN+KaSP sample. Second, since the sample sizes of HUBIN or KaSP were too small to separately form a robust training set and since both samples were acquired on the same scanner, we merged and trained a classifier on HUBIN+KaSP, which was tested on TOP.

Subgroups and Clinical Associations

Since our clinical group included heterogeneous psychosis spectrum patients, we tested for effect of subgroup (98 SZ, 27 SA, 5 SFF, 43 psychosis NOS, 4 brief psychotic disorder, and 6 delusional disorder) on the connectivity of edges showing main effects of diagnosis, covarying for age, sex and site. We also tested for associations with DDD and duration of illness within all patients on any significant edges identified in the main analysis, with age, sex and site as covariates. Associations with total PANSS were tested in TOP+KaSP.

Results

Univariate Connectivity Analysis

Components largely clustered into 7 groups, broadly representing parietal, frontoparietal and cingulum, subcortical, somatosensory and auditory, DMN, frontotemporal, and visual components (supplementary figure S3). Fourteen edges showed significant effect of diagnosis at the Bonferroni-level ($P < .00003$) and 72 edges at the FDR-level ($P < .002$) (figure 1, figure 2A). Bonferroni-corrected edges showed either a reduced magnitude of positive or negative regularized partial correlation (*r* approaching 0) in patients and involved primarily sensory, subcortical, and frontal nodes.

Within the visual networks 2 edges showed decreased positive correlation in patients (IC17-IC36 and IC17-24), and one edge showed reduced magnitude of negative correlation (IC3-IC19) (table 2, figure 2). Two edges involving somatomotor nodes (IC4-IC7 and IC7-IC11) showed reduced positive correlations, and a lateral somatomotor node (IC1) showed reduced negative correlation with a precuneus node (IC48). For the auditory components, IC2 showed reduced positive correlation in patients with IC33 (bilateral middle/superior temporal gyrus) and reduced negative correlation with IC46 (right frontal pole). Subcortically, a thalamus node (IC32) showed reduced negative correlation with bilateral middle/superior temporal gyrus (IC33), and putamen (IC5) showed decreased positive correlation with 2 premotor nodes (IC23 and IC30).

Frontal regions showed decreased positive correlation between 2 nodes reflecting the superior frontal gyrus (IC45) and left inferior frontal gyrus (IC28). A left frontal-parietal node (left middle/inferior frontal gyrus and superior parietal lobule, IC20) and right inferior frontal gyrus (IC37) showed reduced positive correlation in patients. Within the DMN cluster, a precuneus node (IC48) showed reduced positive correlation with a medial frontal node (cingulate, paracingulate, and the frontal pole, IC35).

The directions of effects for the significant edges were the same in all samples (supplementary table S2 and figure 2C). All identified edges were significant ($P < .05$, uncorrected) within TOP, and in the combined HUBIN+KaSP sample all but 3 (IC2-IC33, $P = .105$, IC2-IC46, $P = .133$, and IC20-IC37, $P = .065$) were significant. Within KaSP and HUBIN, 6 and 8 of the 14 edges showed nominally significant effects, respectively.

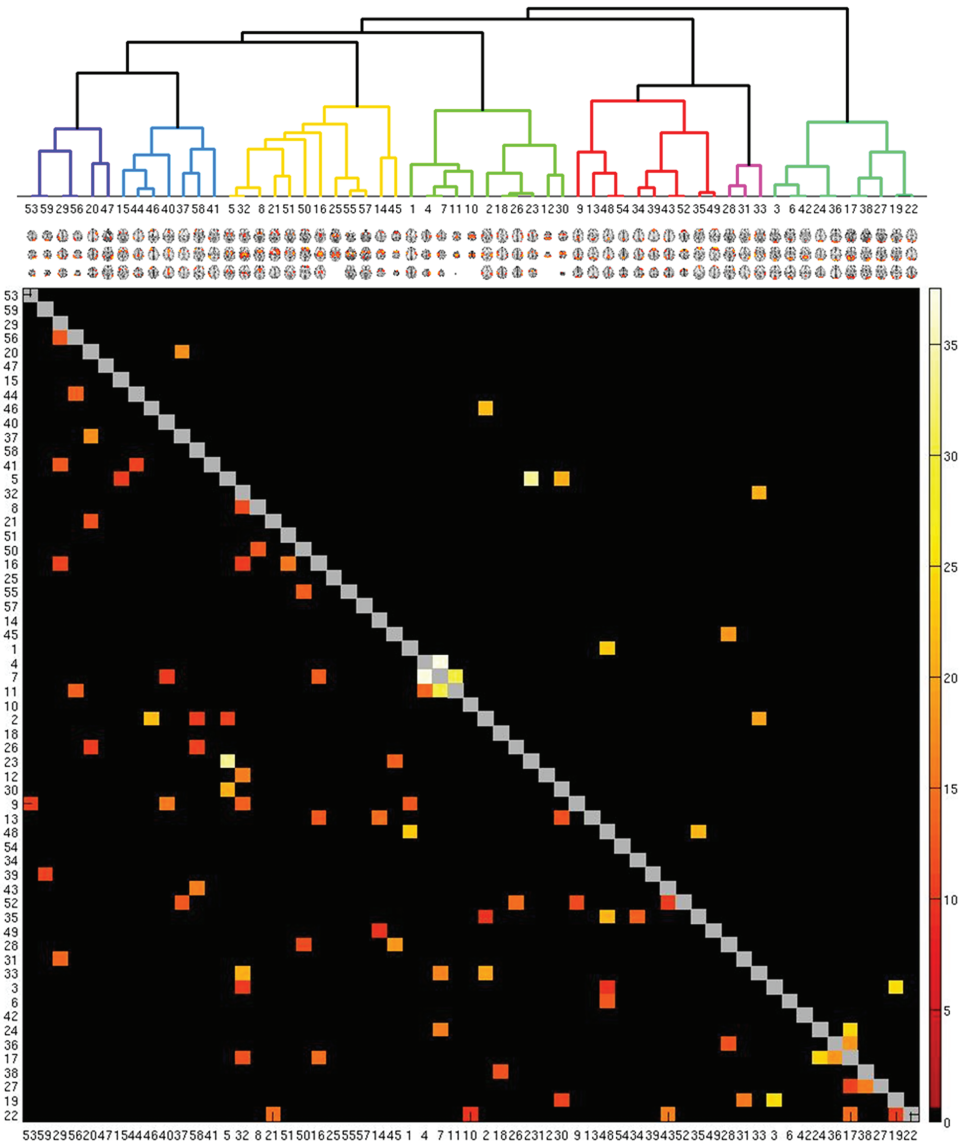

Fig. 1. Effect of group on functional connectivity. Colored squares depict edges with a significant effect of group, represented as *F*-values. Upper triangle shows Bonferroni corrected edges ($P < .00003$), while lower triangle show FDR-corrected edges ($P < .0021$). Cluster colors broadly represents parietal (dark blue), frontoparietal/cingulum (blue), subcortical (yellow), somatomotor/auditory (light green), default mode (red), frontotemporal (pink), and visual/occipital components (green).

Node-wise Eigenvector Centrality Based on Edge-wise Effect Sizes

The highest centrality nodes were IC17 (visual), and IC24 (V2 and cuneus), IC22 (lateral occipital and parietal cortex), IC11 (medial somatomotor), IC39 (medial frontal), and IC28 (left inferior frontal gyrus; supplementary table S3). Of the DMN components, 2 medial frontal and precuneus/cingulate ICs (IC35, IC39, and IC9) also showed high centrality, while frontoparietal, and salience ICs showed average or below average centralities.

Multivariate Analysis—Machine Learning

A classifier trained on TOP showed an overall discrimination accuracy of patients and controls on the combined HUBIN+KaSP sample of 76.7% (sensitivity 80.3%, specificity 73.2%; figure 3). Testing the same classifier only on HUBIN showed an accuracy of 78.3%, with the largest sensitivity of 88.2% (specificity 68.3%), while testing on KaSP showed an accuracy of 77.5% (sensitivity 80%, specificity 75%). Training the classifier on HUBIN and KaSP combined and testing on TOP gave an accuracy of 69% (sensitivity 63.5%, specificity 74.4%).

Subgroups, Clinical Associations, and Motion

Two of the significant edges showed a nominally significant difference between subgroups; IC35-IC48 ($F = 2.76$, $P = .02$) and IC5-IC23 ($F = 2.37$, $P = .041$). Post hoc analysis showed that edge IC48-IC35 had lower positive correlations in SZ and psychosis NOS compared to SA, while SFF had the lowest values

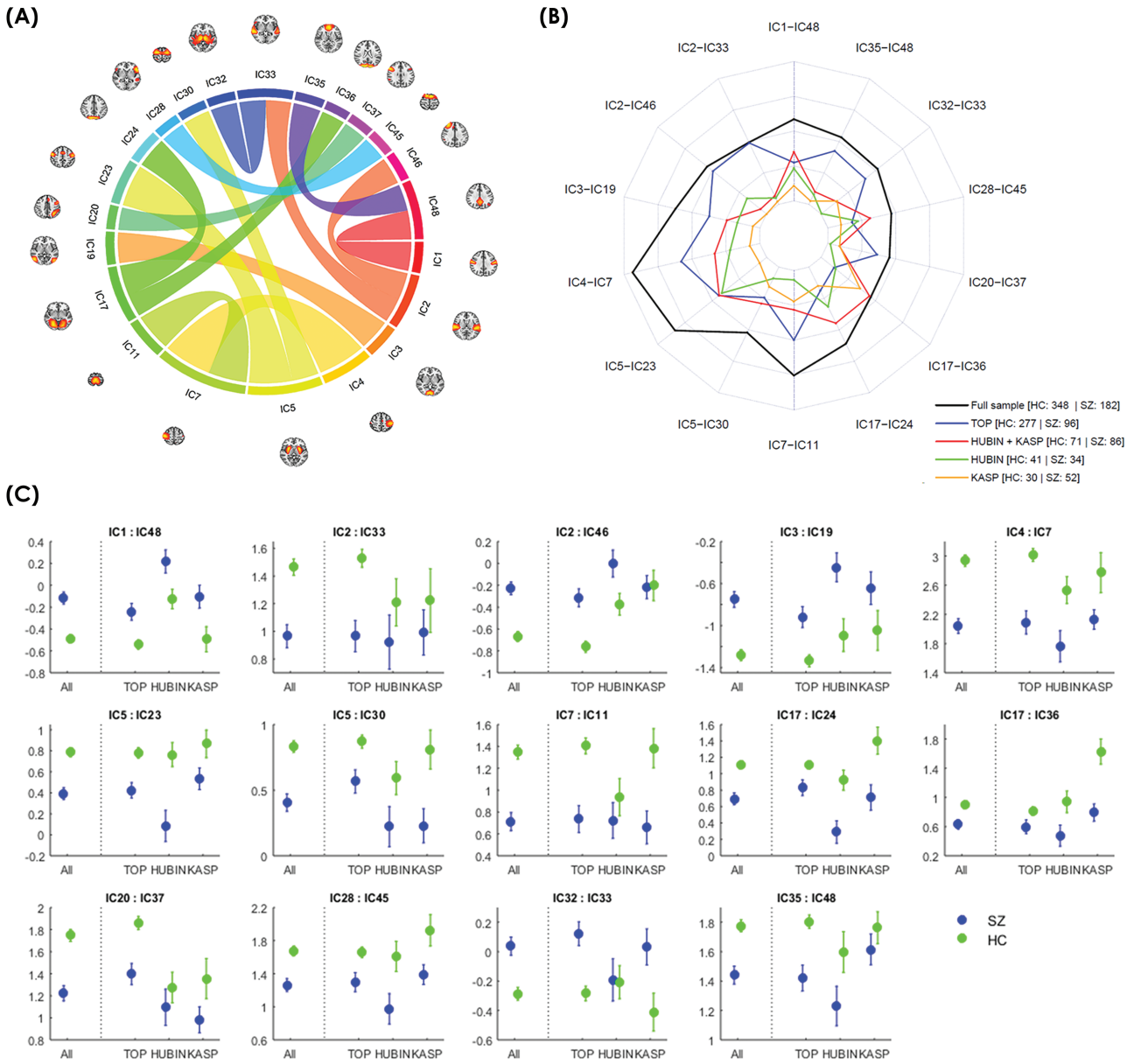

Fig. 2. (A) Correlations and their location between the 14 edges showing an effect of group. (B) Spider plot displaying the *F*-values for the group differences for each significant edge for the different samples. (C) Plots displaying the mean and standard error for all samples.

among the subgroups (supplementary figure S4). SZ, SA, and psychosis NOS had lower correlations for IC5-IC23 compared to SFF, brief psychotic disorder and delusional patients.

Among significant edges from the main analysis, one (IC2-IC46) showed a nominal association with DDD ($F = 4.16$, $t = -2.04$, $P = .044$), with an increasing negative correlation with increasing dose. No edges were associated with total PANSS or duration of illness.

Patients had more head motion than HC, and a greater proportion of noise removed by FIX (supplementary table S1). All 14 edges remained significant after including motion as a covariate, although 4 of the edges were no longer significant at the Bonferroni-level (supplementary table S4). Repeated measures ANOVA showed a large effect of FIX on tSNR, with mean increases from 175.3 to 253.4 ($F = 5616.1$, $P < .001$) (supplementary table S1 and supplementary figure S5). There was no interaction between group and FIX ($F = 1.88$, $P = .172$), though SZ had lower tSNR than HC ($F = 19.2$, $P < .001$). tSNR was associated with functional connectivity within the control group in 5 of 14 edges (nominal $P < .05$) (supplementary table S5). Four of these edges showed increasing connectivity with increasing tSNR, and 1 showed increasing connectivity with decreasing tSNR. Adding tSNR to the main model did not remove any of the group differences (supplementary table S5).

Table 2. Statistics of 14 Edges Significant at the Bonferroni-Level With Effect of Diagnosis on Connectivity

	SZ		HC		ANOVA		
Edge	Mean	SD	Mean	SD	*F*	*P*	Partial η
IC1-IC48	−0.12	0.74	−0.49	0.71	23.42	.0000017	0.039
IC2-IC33	0.97	1.13	1.46	1.10	19.72	.0000109	0.034
IC2-IC46	−0.23	0.78	−0.67	0.83	21.86	.0000037	0.036
IC3-IC19	−0.75	1.00	−1.28	0.98	24.84	.0000008	0.042
IC4-IC7	2.04	1.36	2.94	1.44	37.51	<.0000001	0.061
IC5-IC23	0.39	0.77	0.79	0.81	33.65	<.0000001	0.055
IC5-IC30	0.41	0.91	0.83	0.83	20.89	.0000061	0.036
IC7-IC11	0.71	1.12	1.35	1.19	30.12	.0000001	0.051
IC17-IC24	0.69	0.98	1.11	0.84	24.44	.0000010	0.042
IC17-IC36	0.63	0.89	0.90	1.00	18.25	.0000230	0.032
IC20-IC37	1.22	0.93	1.75	1.02	18.14	.0000243	0.030
IC28-IC45	1.26	1.05	1.67	1.08	18.71	.0000182	0.033
IC32-IC33	0.04	0.83	−0.29	0.81	20.74	.0000065	0.037
IC35-IC48	1.44	0.82	1.78	0.76	21.35	.0000048	0.037

Note: HC, healthy controls; SZ, schizophrenia. See corresponding figures 1 and 2.

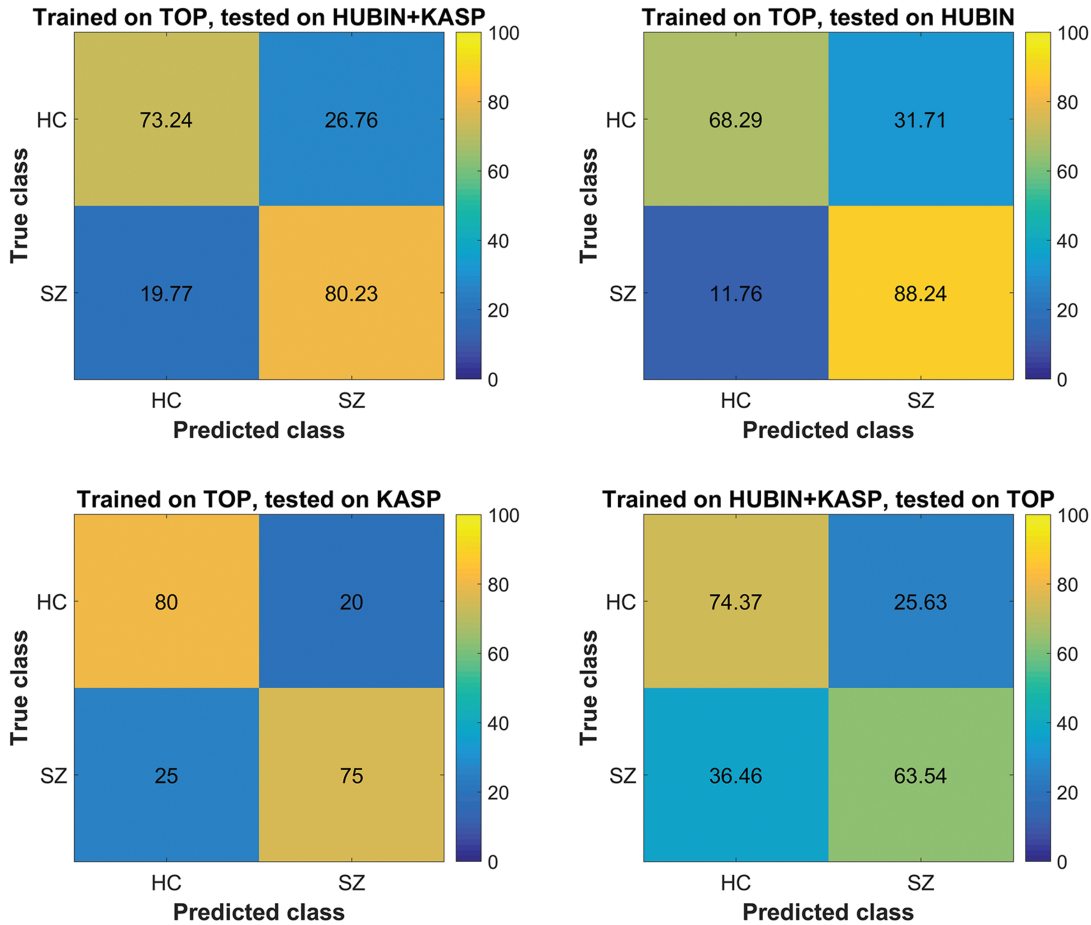

Fig. 3. Functional connectivity based classification of patients and controls, where the classifier is trained on one group and tested on data from another group. HC, healthy controls; SZ, schizophrenia.

Discussion

We have performed a comprehensive brain imaging investigation of functional connectivity in a large cohort of SZ and HC from 3 different samples, numbering a total of 530 subjects. Data-driven definitions of nodes in combination with regularized partial temporal correlation

analysis revealed reduced connectivity in SZ in frontal, sensory, and subcortical networks, which was consistent in all 3 samples. Moreover, training a multivariate classifier on the TOP sample resulted in an accuracy close to 80% in HUBIN+KaSP sample, supporting that the clinical sensitivity of the brain network connectivity measures is generalizable across samples and scanners. Effect of medication, symptom scores, duration of illness, diagnostic subgroups, subject motion, and tSNR were negligible and had very limited effect on the identified group differences. The strengths of the study include a large sample size across 3 different sites and reducing methodological variability by using the same pipeline, which points to similar findings even with diverse patient groups. Classification accuracies were performed in independent samples, thus testing for generalizability across sites, adding to the value of our study. Also, by using a data-driven approach with partial correlations, our study assesses putatively direct connections without the need to impose any predefined neuroanatomical constraints or assumptions.

Strikingly, all connections with a main effect of diagnosis showed a weaker positive or negative correlation in patients, ie, a correlation closer to zero, which can be interpreted as a desynchronization. The frontal lobe is critical for cognitive functions such as planning and problem solving, and has been shown to exhibit reduced connectivity in SZ.[5,26] Several of the edges showing group differences involved frontal nodes, 2 of which also showed high centrality, indicating strong cumulative effect of diagnosis also beyond the edges surviving strict correction for multiple comparisons. We identified reduced connectivity between a medial frontal node and the precuneus, part of the DMN. These regions also showed a high centrality, indicating they are implicated in many edges in SZ, supporting our hypothesis and a role of the DMN in SZ.[63,64] Although the frontal lobe and DMN showed altered connectivity, we did not observe any altered connections directly between the DMN and typical task-positive networks (such as the frontal-parietal network, IC20), which is in contrast to the conception that altered or even opposite correlation patterns between these networks give rise to clinical symptoms.[28]

In line with our hypothesis, sensory networks were particularly affected, with 5 visual nodes showing reduced connectivity with other visual nodes. Three nodes represented early visual cortices (IC36, IC24, and IC3), 2 of which had reduced connectivity with V4 (IC17) and 1 that had reduced connectivity with V5 (IC19). The ventral stream goes through V4 towards the inferior temporal cortex, and is critical for object recognition, visual perception and memory, and the dorsal stream passes through V5 (visual motion). Jointly, these findings demonstrate that both visual processing paths are affected, which further strengthen the conception of dysfunctional multi-level visual information processing in SZ.[16,17]

Three somatomotor regions showed reduced connectivity in patients, which have also been implicated using different approaches.[13,14,16,17] In line with widely documented sensory processing deficits in SZ, both visual and somatosensory nodes had a high centrality, indicating many altered edges involving sensory nodes in patients. The auditory node showed altered connectivity with bilateral temporal and right frontal regions. Auditory processing impairments have been documented in SZ,[65] and auditory hallucinations are one of the core symptoms in SZ.[66] Disrupted flow of information between the auditory cortex and other regions is a candidate mechanism that may manifest as altered functional connectivity patterns. Together, these findings support that sensory processing deficits are a hallmark of SZ. If the quality of the sensory input is already degraded before being forwarded to higher-level processes involving the frontal lobe, it could partially explain the cognitive difficulties observed in SZ. As of today, with some notable exceptions,[13–15] neuroimaging studies have primarily targeted the DMN and cognitive processes, while our results suggest more attention should be given to characterize sensory processing deficits.

Several recent studies have showed disrupted subcortical connectivity, particular between the thalamus and somatomotor and frontal regions.[25,67,68] We extend these findings by documenting reduced thalamo-temporal connectivity in all 3 samples, and decreased connectivity between the putamen and 2 premotor nodes. As the basal ganglia motors circuit involves the thalamus, putamen, and premotor cortex,[69] these findings may indicate poorer coordination of cortico-basal ganglia pathways and subsequent reduced motor function,[70] and also supports our hypothesis of disruptions in the cortico-striatal-thalamic loop.

The group effects for the 14 significant edges were in the same direction in all 3 samples with comparable effect sizes across edges, supporting the robustness of the findings. Six and 8 of the effects were replicated within KaSP and HUBIN, respectively, despite smaller sample sizes, which may also explain some of the discrepancies in the literature.[26] Also, effects of diagnostic subgroup were nominal only and restricted to 2 of the significant edges, suggesting common functional brain pathology across the SZ spectrum.

Using machine learning utilizing all edges we found high overall classification accuracies. Training the classifier on TOP gave good accuracies in KaSP+HUBIN, and even in the smaller individual samples. Training the classifier on KaSP+HUBIN gave slightly lower accuracy in TOP, likely due to a smaller sample size. These robust validations are important since they suggest generalizability of connectivity aberrations across different scanners and heterogeneous samples, including both recently diagnosed and chronic patients. Consequently, our results suggest that a mega-analysis attempt similar to those recently

deployed in the structural imaging domain[71,72] and genetics[73] may be feasible for functional connectivity analysis.

In-scanner head motion may be a confounder as patients moved more than controls. However, we carefully denoised the data using FIX and by regressing out motion parameters, and the main effects of group on edgewise connectivity remained after adding motion as a covariate. FIX substantially increased tSNR across groups, though patients had lower tSNR than HC both before and after FIX. Some edges were associated with tSNR in HC, and mainly showed decreased connectivity with decreasing tSNR. However, adding tSNR to the main model as a covariate did not remove any of the significant group effects, and is therefore unlikely to explain the group differences.

Many patients were treated with antipsychotic medication at the time of scanning, which is a limitation of this study. It is difficult to disentangle the effects of medication and disease mechanisms in naturalistic clinical studies, though effects were found in KaSP where about half of the patients were not medicated. Moreover, the one edge that showed an effect of medication was in the opposite direction of the patient-control difference, making it unlikely that our findings are purely a result of medication effects. Whereas the observed connectivity differences between cases and controls are likely to reflect relevant pathophysiological mechanisms,[74] the links between functional connectivity and clinical, cognitive and behavioral traits are complex[75] and should be interpreted with caution.

In conclusion, we have shown altered functional connectivity encompassing frontal, somatomotor, visual, auditory, and subcortical brain nodes in patients with SZ in 3 different samples. Results were robust across scan sites, with good classification accuracies in the independent samples. Most affected edges involved sensory nodes, corroborating the conception that sensory and perceptual processing may lie at the core of SZ pathophysiology.

Supplementary Material

Supplementary data are available at *Schizophrenia Bulletin* online.

Funding

This work was supported by the Research Council of Norway (204966/F20, 223273, 213837); the South-Eastern Norway Regional Health Authority (2015-073, 2012-047, 2013-123, 2014-097); European Community's 7th Framework Programme (602450, IMAGEMEND), and Kristian Gerhard Jebsen Foundation (SKGJ-MED-008). HUBIN was supported by the Swedish Research Council (K2007-62X-15077-04-1, K2008-62P-20597-01-3, K2010-62X-15078-07-2, K2012-61X-15078-09-3), the regional agreement on medical training and clinical research between Stockholm County Council, the Karolinska Institutet, and the Knut and Alice Wallenberg Foundation. The KaSP consortium was supported by grants from the Swedish Research Council (2011-4730 and samverkansanslag), the Stockholm County Council (ALF 20090192, ALF 20140469, ALF 20150475) and the Centre for Psychiatric Research (CPF 100/2011) Swedish Medical Research Council (2009-7053; 2013-2838), the Swedish Brain Foundation, Söderström Königska, and Torsten Söderbergs Stiftelse.

Acknowledgments

We thank the study participants and our collaborators at NORMENT, KaSP, and HUBIN, the staff at the Department of Radiology and Nuclear Medicine at Ullevål Hospital in Oslo, and at the MR-centre at the Karolinska Hospital in Sweden. *Collaborators*: Members of the Karolinska Schizophrenia Project (KaSP) at Karolinska Institutet, Stockholm, Sweden. Department of Clinical Neuroscience: Farde L., Flyckt L., Fatouros-Bergman H., Piehl F., Cervenka S., Agartz I., Ikonen P., and Collste K. Department of Physiology and Pharmacology: Malmqvist A., Hedberg M., Engberg G., Erhardt S., Schwieler L., and Orhan F. O.A.A. has received a speakers honorarium from Lilly, Otsuka, Lundbeck. The other authors declare no conflict of interest.

References

1. van Os J, Kapur S. Schizophrenia. *Lancet*. 2009;374:635–645.
2. Friston KJ, Frith CD. Schizophrenia: a disconnection syndrome? *Clin Neurosci*. 1995;3:89–97.
3. Owen MJ, Sawa A, Mortensen PB. Schizophrenia. *Lancet*. 2016;388:86–97.
4. van den Heuvel MP, Scholtens LH, de Reus MA, Kahn RS. Associated microscale spine density and macroscale connectivity disruptions in schizophrenia. *Biol Psychiatry*. 2016;80:293–301.
5. Fornito A, Zalesky A, Pantelis C, Bullmore ET. Schizophrenia, neuroimaging and connectomics. *Neuroimage*. 2012;62:2296–2314.
6. Romme IAC, De Reus MA, Ophoff RA, Kahn RS, Van den Heuvel M. Connectome disconnectivity and cortical gene expression in schizophrenia [published online ahead of print July 27, 2016]. *Biol Psychiatry*.
7. Skåtun KC, Kaufmann T, Tonnesen S, et al. Global brain connectivity alterations in patients with schizophrenia and bipolar spectrum disorders. *J Psychiatry Neurosci*. 2016;41:150159.
8. Garrity AG, Pearlson GD, McKiernan K, Lloyd D, Kiehl KA, Calhoun VD. Aberrant "default mode" functional connectivity in schizophrenia. *Am J Psychiatry*. 2007;164:450–457.
9. Jiang T, Zhou Y, Liu B, Liu Y, Song M. Brainnetome-wide association studies in schizophrenia: the advances and future. *Neurosci Biobehav Rev*. 2013;37:2818–2835.
10. Sridharan D, Levitin DJ, Menon V. A critical role for the right fronto-insular cortex in switching between central-executive

and default-mode networks. *Proc Natl Acad Sci U S A*. 2008;105:12569–12574.

11. Uddin LQ. Salience processing and insular cortical function and dysfunction. *Nat Rev Neurosci*. 2015;16:55–61.
12. Northoff G, Duncan NW. How do abnormalities in the brain's spontaneous activity translate into symptoms in schizophrenia? From an overview of resting state activity findings to a proposed spatiotemporal psychopathology [published online ahead of print August 12, 2016]. *Prog Neurobiol*.
13. Berman RA, Gotts SJ, McAdams HM, et al. Disrupted sensorimotor and social-cognitive networks underlie symptoms in childhood-onset schizophrenia. *Brain*. 2016;139:276–291.
14. Kaufmann T, Skåtun KC, Alnæs D, et al. Disintegration of sensorimotor brain networks in schizophrenia [published online ahead of print May 4, 2015]. *Schizophr Bull*.
15. Liemburg EJ, Vercammen A, Ter Horst GJ, Curcic-Blake B, Knegtering H, Aleman A. Abnormal connectivity between attentional, language and auditory networks in schizophrenia. *Schizophr Res*. 2012;135:15–22.
16. Butler PD, Silverstein SM, Dakin SC. Visual perception and its impairment in schizophrenia. *Biol Psychiatry*. 2008;64:40–47.
17. Javitt DC. Sensory processing in schizophrenia: neither simple nor intact. *Schizophr Bull*. 2009;35:1059–1064.
18. Javitt DC, Freedman R. Sensory processing dysfunction in the personal experience and neuronal machinery of schizophrenia. *Am J Psychiatry*. 2015;172:17–31.
19. Revheim N, Corcoran CM, Dias E, et al. Reading deficits in schizophrenia and individuals at high clinical risk: relationship to sensory function, course of illness, and psychosocial outcome. *Am J Psychiatry*. 2014;171:949–959.
20. Andreasen NC. The role of the thalamus in schizophrenia. *Can J Psychiatry*. 1997;42:27–33.
21. Cromwell HC, Mears RP, Wan L, Boutros NN. Sensory gating: a translational effort from basic to clinical science. *Clin EEG Neurosci*. 2008;39:69–72.
22. Bak N, Rostrup E, Larsson HB, Glenthøj BY, Oranje B. Concurrent functional magnetic resonance imaging and electroencephalography assessment of sensory gating in schizophrenia. *Hum Brain Mapp*. 2014;35:3578–3587.
23. Tregellas JR, Davalos DB, Rojas DC, et al. Increased hemodynamic response in the hippocampus, thalamus and prefrontal cortex during abnormal sensory gating in schizophrenia. *Schizophr Res*. 2007;92:262–272.
24. Cheng W, Palaniyappan L, Li M, et al. Voxel-based, brain-wide association study of aberrant functional connectivity in schizophrenia implicates thalamocortical circuitry. *NPJ Schizophr*. 2015;1:15016.
25. Woodward ND, Karbasforoushan H, Heckers S. Thalamocortical dysconnectivity in schizophrenia. *Am J Psychiatry*. 2012;169:1092–1099.
26. Pettersson-Yeo W, Allen P, Benetti S, McGuire P, Mechelli A. Dysconnectivity in schizophrenia: where are we now? *Neurosci Biobehav Rev*. 2011;35:1110–1124.
27. Su TW, Hsu TW, Lin YC, Lin CP. Schizophrenia symptoms and brain network efficiency: a resting-state fMRI study. *Psychiatry Res*. 2015;234:208–218.
28. Sheffield JM, Barch DM. Cognition and resting-state functional connectivity in schizophrenia. *Neurosci Biobehav Rev*. 2016;61:108–120.
29. Ekholm B, Ekholm A, Adolfsson R, et al. Evaluation of diagnostic procedures in Swedish patients with schizophrenia and related psychoses. *Nord J Psychiatry*. 2005;59:457–464.
30. Kay SR, Fiszbein A, Opler LA. The positive and negative syndrome scale (PANSS) for schizophrenia. *Schizophr Bull*. 1987;13:261–276.
31. Andreasen NC. *Scale for the Assessment of Positive Symptoms (SAPS)*. Iowa City, IA: University of Iowa; 1984.
32. Andreasen NC. The Scale for the Assessment of Negative Symptoms (SANS): conceptual and theoretical foundations. *Br J Psychiatry Suppl*. 1989;7:49–58.
33. Spitzer RL, Williams JBW, Kroenke K, et al. Utility of new procedure for diagnosing mental-disorders in primary-care - the Prime-MD-1000 Study. *JAMA J Am Med Assoc*. 1994;272:1749–1756.
34. Spitzer RL, Williams JBW, Gibbon M. *Structured Clinical Interview forDSM-III-R — Non-patient Version (SCID-NP)*. New York, NY: New York States Psychiatric Institute. Biometrics Research Department; 1986.
35. Sheehan DV, Lecrubier Y, Sheehan KH, et al. The Mini-International Neuropsychiatric Interview (M.I.N.I.): the development and validation of a structured diagnostic psychiatric interview for DSM-IV and ICD-10. *J Clin Psychiatry* 1998;59(suppl 20):22–33;quiz 34–57.
36. Salimi-Khorshidi G, Douaud G, Beckmann CF, Glasser MF, Griffanti L, Smith SM. Automatic denoising of functional MRI data: combining independent component analysis and hierarchical fusion of classifiers. *Neuroimage*. 2014;90:449–468.
37. Griffanti L, Salimi-Khorshidi G, Beckmann CF, et al. ICA-based artefact removal and accelerated fMRI acquisition for improved resting state network imaging. *Neuroimage*. 2014;95:232–247.
38. Pruim RH, Mennes M, Buitelaar JK, Beckmann CF. Evaluation of ICA-AROMA and alternative strategies for motion artifact removal in resting state fMRI. *Neuroimage*. 2015;112:278–287.
39. Pruim RH, Mennes M, van Rooij D, Llera A, Buitelaar JK, Beckmann CF. ICA-AROMA: A robust ICA-based strategy for removing motion artifacts from fMRI data. *Neuroimage*. 2015;112:267–277.
40. Roalf DR, Quarmley M, Elliott MA, et al. The impact of quality assurance assessment on diffusion tensor imaging outcomes in a large-scale population-based cohort. *Neuroimage*. 2016;125:903–919.
41. Fischl B, Salat DH, Busa E, et al. Whole brain segmentation: automated labeling of neuroanatomical structures in the human brain. *Neuron*. 2002;33:341–355.
42. Dale AM, Fischl B, Sereno MI. Cortical surface-based analysis. I. Segmentation and surface reconstruction. *Neuroimage*. 1999;9:179–194.
43. Jenkinson M, Beckmann CF, Behrens TE, Woolrich MW, Smith SM. FSL. *Neuroimage*. 2012;62:782–790.
44. Jenkinson M, Bannister P, Brady M, Smith S. Improved optimization for the robust and accurate linear registration and motion correction of brain images. *Neuroimage*. 2002;17:825–841.
45. Greve DN, Fischl B. Accurate and robust brain image alignment using boundary-based registration. *Neuroimage*. 2009;48:63–72.
46. Mazziotta J, Toga A, Evans A, et al. A probabilistic atlas and reference system for the human brain: International Consortium for Brain Mapping (ICBM). *Philos Trans R Soc Lond B Biol Sci*. 2001;356:1293–1322.
47. Biswal BB, Mennes M, Zuo XN, et al. Toward discovery science of human brain function. *Proc Natl Acad Sci U S A*. 2010;107:4734–4739.

48. Beckmann CF, Mackay C, Filippini N, Smith SM. Group comparison of resting-state FMRI data using multi-subject ICA and dual regression. *OHBM*. 2009.
49. Filippini N, MacIntosh BJ, Hough MG, et al. Distinct patterns of brain activity in young carriers of the APOE-epsilon4 allele. *Proc Natl Acad Sci U S A*. 2009;106:7209–7214.
50. Brandt CL, Kaufmann T, Agartz I, et al. Cognitive effort and schizophrenia modulate large-scale functional brain connectivity [published online ahead of print March 1, 2015]. *Schizophr Bull*.
51. Smith SM, Nichols TE, Vidaurre D, et al. A positive-negative mode of population covariation links brain connectivity, demographics and behavior. *Nat Neurosci*. 2015;18:1565–1567.
52. Smith SM, Vidaurre D, Beckmann CF, et al. Functional connectomics from resting-state fMRI. *Trend Cogn Sci*. 2013;17:666–682.
53. Brier MR, Mitra A, McCarthy JE, Ances BM, Snyder AZ. Partial covariance based functional connectivity computation using Ledoit-Wolf covariance regularization. *Neuroimage*. 2015;121:29–38.
54. Marrelec G, Krainik A, Duffau H, et al. Partial correlation for functional brain interactivity investigation in functional MRI. *Neuroimage*. 2006;32:228–237.
55. Fox MD, Zhang D, Snyder AZ, Raichle ME. The global signal and observed anticorrelated resting state brain networks. *J Neurophysiol*. 2009;101:3270–3283.
56. Van Dijk KR, Hedden T, Venkataraman A, Evans KC, Lazar SW, Buckner RL. Intrinsic functional connectivity as a tool for human connectomics: theory, properties, and optimization. *J Neurophysiol*. 2010;103:297–321.
57. Kaufmann T, Elvsashagen T, Alnæs D, et al. The brain functional connectome is robustly altered by lack of sleep. *Neuroimage*. 2016;127:324–332.
58. Schäfer J, Strimmer K. A shrinkage approach to large-scale covariance matrix estimation and implications for functional genomics. *Stat Appl Genet Mol Biol*. 2005;4:Article32.
59. Ledoit O, Wolf M. Improved estimation of the covariance matrix of stock returns with an application to portfolio selection. *J Emp Finance*. 2003;10:603–621.
60. Nichols T, Hayasaka S. Controlling the familywise error rate in functional neuroimaging: a comparative review. *Stat Methods Med Res*. 2003;12:419–446.
61. Friedman JH. Regularized discriminant-analysis. *J Am Stat Assoc*. 1989;84:165–175.
62. Alnæs D, Sneve MH, Richard G, et al. Functional connectivity indicates differential roles for the intraparietal sulcus and the superior parietal lobule in multiple object tracking. *Neuroimage*. 2015;123:129–137.
63. Whitfield-Gabrieli S, Ford JM. Default mode network activity and connectivity in psychopathology. *Annu Rev Clin Psychol*. 2012;8:49–76.
64. Broyd SJ, Demanuele C, Debener S, Helps SK, James CJ, Sonuga-Barke EJ. Default-mode brain dysfunction in mental disorders: a systematic review. *Neurosci Biobehav Rev*. 2009;33:279–296.
65. Javitt DC, Sweet RA. Auditory dysfunction in schizophrenia: integrating clinical and basic features. *Nat Rev Neurosci*. 2015;16:535–550.
66. Hugdahl K. "Hearing voices": auditory hallucinations as failure of top-down control of bottom-up perceptual processes. *Scand J Psychol*. 2009;50:553–560.
67. Anticevic A, Cole MW, Repovs G, et al. Characterizing thalamo-cortical disturbances in schizophrenia and bipolar illness. *Cereb Cortex*. 2014;24:3116–3130.
68. Skåtun KC, Kaufmann T, Brandt CL, et al. Thalamo-cortical functional connectivity in schizophrenia and bipolar disorder. Submitted.
69. DeLong MR, Wichmann T. Circuits and circuit disorders of the basal ganglia. *Arch Neurol*. 2007;64:20–24.
70. Bracht T, Schnell S, Federspiel A, et al. Altered cortico-basal ganglia motor pathways reflect reduced volitional motor activity in schizophrenia. *Schizophr Res*. 2013;143:269–276.
71. van Erp TG, Hibar DP, Rasmussen JM, et al. Subcortical brain volume abnormalities in 2028 individuals with schizophrenia and 2540 healthy controls via the ENIGMA consortium [published online ahead of print June 2, 2015]. *Mol Psychiatry*.
72. Hibar DP, Stein JL, Renteria ME, et al. Common genetic variants influence human subcortical brain structures. *Nature*. 2015;520:224–229.
73. Thompson PM, Stein JL, Medland SE, et al. The ENIGMA Consortium: large-scale collaborative analyses of neuroimaging and genetic data. *Brain Imaging Behav*. 2014;8:153–182.
74. Yang GJ, Murray JD, Wang XJ, et al. Functional hierarchy underlies preferential connectivity disturbances in schizophrenia. *Proc Natl Acad Sci U S A*. 2016;113:E219–228.
75. Deco G, Jirsa VK, McIntosh AR. Resting brains never rest: computational insights into potential cognitive architectures. *Trends Neurosci*. 2013;36:268–274.